Sensing and Imaging (2019) 20:1
https://doi.org/10.1007/s11220-018-0222-y

ORIGINAL PAPER

Modeling and Enhancement of Piezoelectric Accelerometer Relative Sensitivity

Salima Khaoula Reguieg[1] · Zine Ghemari[1] · Tarak Benslimane[1] · Salah Saad[2]

Received: 29 August 2018 / Revised: 4 October 2018

Abstract

The piezoelectric accelerometer is an electronic instrument based on the direct effect of the piezoelectric material, this device is widely used in the industries to monitor and detect defects of rotating machines in an early stage. In this paper, a thorough study of the piezoelectric accelerometer is carried out to understand its design and operation principle. A mathematical model of the accelerometer is developed based on Newton motion law then a new relative sensitivity equation in function of measurement error is extracted. This new equation has allowed a significant reduction in the measurement error, a maximum improvement in the precision and an optimization of the piezoelectric accelerometer relative sensitivity by the appropriate choice of damping rate. These improvements have optimized the accelerometer parameters and performances.

Keywords Model · Error · Measurement · Sensitivity · Accelerometer

List of Symbols

ω	The relative frequency
ω_0	The natural frequency
ξ	The damping rate
m	The mass
c	The damping factor
k	The elasticity coefficient
y	The absolute motion
z	The relative vibratory motion
S_1	The mechanical sensitivity
γ	The acceleration
E	The measurement error

✉ Zine Ghemari
zine.ghemari@univ-msila.dz

1 Electrical Engineering Laboratory, Mohamed Boudiaf University of M'sila, M'sila, Algeria

2 University of Badji Mokhtar, Annaba 23000, Algeria

Published online: 04 December 2018

Q The electric charge
S The sensitivity
C The accelerometer internal impedance
R The insulation resistance
S_2 The electrical sensitivity
S_r Relative sensitivity

1 Introduction

Machines monitoring relies essentially on the extraction of information revealing the encountered degradation conditions. Several sources of information have been explored and tested in the past, with more or less efficiency. Among these we cite oil analysis, temperature analysis, acoustic emission and vibratory analysis with higher intensity.

Vibration analysis plays a major role in the detection and diagnosis of defects in rotating machines, and this is increasing, because of the ever increasing performance in signal processing. The acquisition of vibratory information is done in several steps. The first, the transformation of the mechanical displacements into an electrical signal by means of sensors installed on the machine, followed by signals acquisition and sampling (conventionally at constant time step) in order to be processed by computing devices. The final step is the signals digital processing in order to extract information useful for the recognition of operating states [1, 2].

The vibratory analysis method is composed from a series of elements such as the accelerometer, the amplifier and the FFT analyzer. The accelerometer transforms the vibratory motion into a temporal electrical signal, the amplifier amplifies the signal and the FFT analyzer converts the temporal electrical signal into a frequency electric signal (frequency information) [3–6].

In this work, the piezoelectric accelerometer is chosen because of it has many advantages compared to other types of accelerometers (capacitive, resistive, tunnel effect…). The piezoelectric accelerometer is based on the piezoelectric effect and the piezoelectricity is the ability of certain crystalline materials to produce an electrical charge proportional to the mechanical stress. The application of an external electric field causes a mechanical deformation; this phenomenon is called inverse piezoelectric effect.

Several research studies were conducted in order to improve the performance of the piezoelectric accelerometer especially the electrical part [7–17]. However, the study of Hu et al. [18] introduces a piezoelectric sensor based on vortex-induced vibrations. This sensor module is endowed with a piezoelectric cantilever and cylinder, which can be used to measure the wind flow from the characteristic of vortex signals. The application potential for the on-line detection of partial discharges of a new generation of piezoelectric sensors (High Temperature Ultrasonic Transducers, HTUTs) is presented in [19]. Such sensor was recently developed by Canada's Industrial Materials Institute (IMI). The proposed sensor system in [20] consists of a piezoelectric energy harvesting device and a signal conditioning circuit. This device is used to sense and convert ambient vibration to

a relevant output voltage. The signal conditioning circuit, designed by a Bias-Flip circuit, a pulse shaper and a low pass filter are employed to generate a DC output voltage which is proportional to the vibration frequency magnitude.

However, in the present work, a mathematical model suitable to the piezoelectric accelerometer will be developed and proposed. With this model it will be possible to optimize the sensor relative sensitivity, to minimize the measurement error and to improve the accuracy. These improvements in the characteristics and in the parameters make possible to propose a new design of piezoelectric accelerometer with higher precision and reliability.

2 Research Methodology

In the piezoelectricity section, the piezoelectric material direct effect is explained, and in the piezoelectric accelerometer section, this type of sensor is described with their operating principle, then in the accelerometer modeling section, the mathematical model of the accelerometer physical behavior (mechanical and electrical model) is extracted. Finally, in the results analysis section, the developed model is validated and confirmed by simulation. The obtained results are analyzed and discussed before a conclusion is drawn.

3 Piezoelectricity

The piezoelectricity phenomenon is observed naturally in crystals quartz. In the absence of deformation, the crystal remains electrically neutral. Under the effect of a mechanical action, an electric dipole appears in each mesh of the material by displacement of the barycenter's positive and negative charges. The application of a mechanical action on one of the faces of a piezoelectric sample breaks its natural electrostatic balance and causes the appearance of an electric field at its terminals (see Fig. 1).

The sum of elementals electric fields gives birth to a macroscopic electric field. The piezoelectric materials are able to generate electrical charges on certain faces of the sample under the effect of an external mechanical stress (whatever the internal constraints of the existing material before the presence of external effort). This effect is called direct piezoelectric effect and is used in the manufacture of force, pressure, acceleration sensors and others. On the other hand, when a voltage is applied across two opposite faces, the produced electric field causes the appearance of a mechanical stress (which results in a shape variation if the sample is free or force if the sample is flush). This property is called reverse effect of piezoelectric. This effect is used for high quartz oscillator frequencies or to make actuators such as sonars or resonators [21].

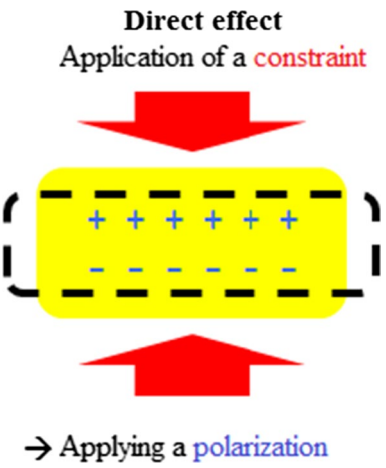

Fig. 1 Direct effect of the piezoelectric materials

4 Description of Piezoelectric Accelerometer

Generally, the piezoelectric accelerometer converts a mechanical deformation (charge or mechanical force) into a temporal electrical signal (the direct effect of piezoelectricity). In this type of sensor, the vibration measurement is based on the deformation of the piezoelectric material. This material is characterized by two parameters, the electromechanical torque k and the piezoelectric constant d [21]. The main advantages of these materials reside in the excellent piezoelectric property, a high coefficient of electromechanical coupling which leads to high efficiency of actuation and high linearity of properties. The composition of the piezoelectric accelerometer is shown in the following figure (Fig. 2).

In the piezoelectric accelerometer, the seismic mass is supported by a piezoelectric element, which delivers an electric charge proportional to the restoring force, and therefore to the displacement of the seismic mass. The assembly is secured by a rigid base, the whole being contained in a hermetic housing.

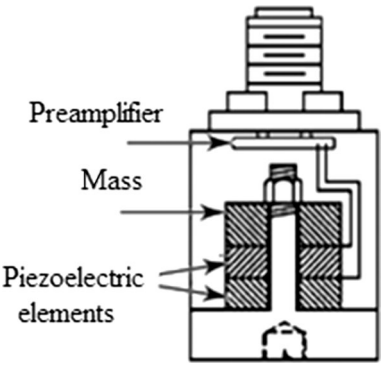

Fig. 2 Piezoelectric accelerometer structure

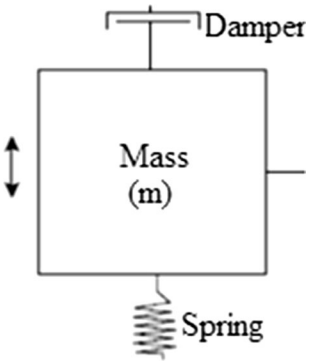

Fig. 3 Mass, spring and damper system

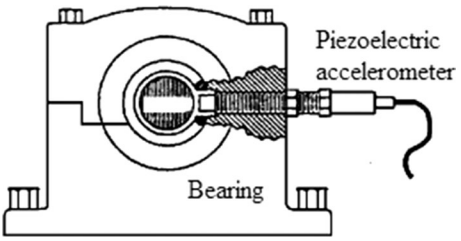

Fig. 4 Implantation of piezoelectric accelerometer

5 Accelerometer Modeling

In this section, the mechanical and electrical part of the piezoelectric accelerometer will be modeled and the accelerometer modeling is presented as follows:

5.1 Mechanical Model

Accelerometers can be considered as a system with a single degree of freedom as shown in the following figure (Fig. 3).

Implantation of piezoelectric accelerometer is in the main sensor sensitivity direction. It must be closer to the vibrating area of interest (see Fig. 4). Fixing the accelerometer on the structure can have a real influence on the quality of the measured signal. It can be fixed in various ways on the machine: screwed into the structure, screwed on a glued base, magnetic for ferric structures, or attached with a touch point.

The following relation shows the relative motion of the piezoelectric accelerometer (z):

$$z(t) = x(t) - y(t) \tag{1}$$

Applying the first law of motion, we can write the following equation:

$$\sum F = m\gamma = mp^2 z \tag{2}$$

With: p is the Laplace coefficient

The piezoelectric accelerometer is considered as a system composed by mass, spring and damper, then Eq. (2) becomes as follows:

$$mp^2z + cpz + kz = -mp^2y \tag{3}$$

With: m is the mass, c is the damping factor, k is the elasticity coefficient, y is the absolute movement and p^2y is the absolute acceleration.

The natural frequency of the accelerometer can be expressed as a function of the seismic mass and the elasticity coefficient, its expression is illustrated by the following relation:

$$\omega_0 = \sqrt{\left(\frac{k}{m}\right)} \tag{4}$$

The damping rate is the ratio between the damping factor, the seismic mass and the natural frequency, thus; we can write:

$$\zeta = \frac{c}{(2m\omega_0)} \tag{5}$$

ω_0 is the natural frequency and ξ is the damping rate.

By substituting Eqs. (4) and (5) in Eq. (3), the relative motion z is expressed as follows:

$$z = -\frac{yp^2}{p^2 + 2\omega_0 p + \omega_0^2} \tag{6}$$

The Laplace coefficient (p) can be replaced by (jω), Eq. (6) becomes:

$$z = \frac{y\omega^2}{-\omega^2 + 2j\omega\omega_0 + \omega_0^2} \tag{7}$$

ω is the relative frequency of vibratory movement.

Equation (7) can be written as follows:

$$z = \frac{y\omega^2}{\omega_0^2(1 - \left(\frac{\omega}{\omega_0}\right)^2 + \left(\frac{2j\omega}{\omega_0}\right)} \tag{8}$$

Equation (8) is a complex function, its module is:

$$z = \frac{y\omega^2}{\omega_0^2\sqrt{\left(1 - \left(\frac{\omega}{\omega_0}\right)^2\right)^2 + \left(\frac{2\omega}{\omega_0}\right)^2}} \tag{9}$$

This equation illustrates the relative motion of the vibrations measured by the piezoelectric accelerometer.

If we denote by γ the acceleration of the vibratory movement (input quantity) measured by the piezoelectric accelerometer and Q the electric charge (output quantity) therefore, the sensitivity S is written as:

$$S = \frac{Q}{\gamma} = S_1 \cdot S_2 \tag{10}$$

where S_1 is the mechanical sensitivity of the seismic mass system (2^{nd} order response):

$$S_1 = \frac{z}{\gamma} = \frac{1}{\omega_0^2 \sqrt{\left(1 - \left(\frac{\omega}{\omega_0}\right)^2\right)^2 + \left(\frac{2\zeta\omega}{\omega_0}\right)^2}} \tag{11}$$

S_2 is the electrical sensitivity of the sensor (1st order response):

$$|S_2| = \left|\frac{Q}{z}\right| = d \cdot C \frac{1}{\sqrt{1 + \left(\frac{\omega_c}{\omega}\right)^2}} \tag{12}$$

d: the piezoelectric constant; C: the stiffness of the sensitive element ω_c is the low cutoff frequency of the accelerometer + conditioner assembly.

The sensitivity of the accelerometer is:

$$S = \frac{d \cdot C}{\sqrt{1 + \left(\frac{\omega_c}{\omega}\right)^2}} \cdot \frac{1/\omega_0^2}{\sqrt{\left(1 - \frac{\omega^2}{\omega_0^2}\right)^2 + \left(2.\zeta.\frac{\omega}{\omega_0}\right)^2}} \tag{13}$$

The relation of the accelerometer relative sensitivity can be expressed as follows:

$$S_r = \frac{S}{S_m} \tag{14}$$

With:

$$S_m = \frac{d \cdot C}{\omega_0^2} \tag{15}$$

So:

$$S_r = \frac{1}{\sqrt{1 + \left(\frac{\omega_c}{\omega}\right)^2}} \cdot \frac{1}{\sqrt{\left(1 - \frac{\omega^2}{\omega_0^2}\right)^2 + (2.\zeta.\frac{\omega}{\omega_0})^2}} \tag{16}$$

From Eqs. (9 and 16), the new formula of the relative sensitivity as a function of the relative movement is obtained, which is illustrated by the following equation:

$$S_r = \frac{1}{\sqrt{1+\left(\frac{\omega_c}{\omega}\right)^2}} \cdot \frac{z\omega_0^2}{Y\omega^2} \tag{17}$$

The measurement error of the piezoelectric accelerometer has the following expression:

$$E = \frac{\left(d^2y/dt^2\right)}{\left(d^2z/dt^2\right)} - 1 = \left[z \cdot \omega_0^2/y\omega^2\right] - 1 \tag{18}$$

E: the measurement error

Then, from Eq. (9), the measurement error is defined by the following formula:

$$E = \frac{1}{\sqrt{\left(1-(\omega/\omega_n)^2\right)^2 + \left(2\zeta\omega/\omega_n\right)^2}} - 1 \tag{19}$$

The new relation that relates the relative sensitivity according to the measurement error is:

$$Sr = \frac{1}{\sqrt{1+\left(\frac{\omega_c}{\omega}\right)^2}} \cdot (E+1) \tag{20}$$

With this equation, it becomes possible to improve the parameters and propose a new design of the piezoelectric accelerometer.

5.2 Electrical Model

The piezoelectric material of the accelerometer can be considered as a current generator of intensity i = dQ/dt in parallel to internal impedance, the following figure illustrates the diagram of a current generator (Fig. 5).

The corresponding equivalent Thevenin scheme is shown in Fig. 6:

From Fig. 6, the transfer function of this circuit can be extracted as follows:

$$H(j\omega) = \frac{j\omega}{j\omega + 1/RC} \tag{21}$$

With: C is the accelerometer internal impedance and R is the insulation resistance of the piezoelectric material,

The amplitude of this transfer function is:

$$|H(j\omega)| = \frac{\omega}{\sqrt{\omega^2 + (\frac{1}{R.C})^2}} \tag{22}$$

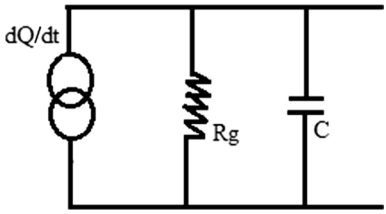

Fig. 5 Current generator of the piezoelectric material

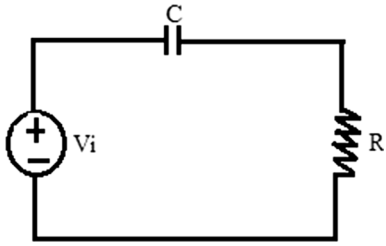

Fig. 6 The equivalent diagram of Thevenin

And the phase shift is given by the following relation:

$$\theta(j\omega) = 90° - tan^{-1}\omega.R.C \tag{23}$$

The cutoff pulse ω_C can be expressed by the formula presented below:

$$\omega_C = \frac{1}{R \cdot C} \tag{24}$$

The insulation resistance of the piezoelectric material is given by the expression:

$$R = \frac{\tan\delta}{2\pi \cdot f \cdot C} = \frac{\tan\delta}{\omega \cdot C} \tag{25}$$

Replacing Eq. (25) in Eq. (24) yields Eq. (26):

$$\omega_C = \frac{\omega}{\tan\delta} \tag{26}$$

The following table shows the parameters of the PZT (PZ27) piezoelectric material (see Table 1)

6 Simulation and Results Interpretation

Simulation refers to the execution of a program on a computer or network in order to simulate a real and complex physical phenomenon. In this work, Matlab software will be used to simulate the developed mathematical model of the mechanical behavior of the piezoelectric accelerometer. In simulation, the accelerometer natural frequency is take equal to 10,000 Hz, the relative frequency is varied from 0 to 4200 Hz (respecting the condition that the maximum relative frequency is smaller compared to the sensor natural frequency to avoid the resonance

Table 1 PZT (PZ27) piezoelectric material parameters

Parameters	Value	Unit
Accelerometer internal impedance (C)	7835 à 1 kHz	pf
Piezoelectric constant (d)	500	pC/N
tan δ	15.85	10^{-3}

phenomenon effect) and the damping rate is varied from 0.6 to 0.7, taking its best value in order to optimize the parameters of the piezoelectric accelerometer. The parameters used to simulate this model are presented in Table 2:

The equations (Eqs. 9, 19 and 20) are used to perform the simulation of relative movement, measurement error, and relative sensitivity of the piezoelectric accelerometer as a function of relative frequency. The simulation results are presented in the following figures (Figs. 7, 8 and 9).

Figure 7 illustrates the relative movement as a function of relative frequency for five damping rate values (0.6, 0.63, 0.65, 0.68, and 0.7). From these five curves, it is observed that there is a difference between these curves because of the damping rate variation. It can also be seen that the damping rate has an effect on the piezoelectric accelerometer accuracy. To extract the appropriate value of damping rate which reduces the measurement error to a minimum, Eq. (19) is simulated.

The simulation of the error equation helps to choose the appropriate damping rate to obtain a more accurate accelerometer (with small measurement error, a high accuracy is obtained). The simulation results are presented in the following figure (Fig. 8).

Figure 8 shows a graphical presentation of the measurement error as a function of relative movement frequency for five values of damping rate (0.6, 0.63, 0.65, 0.68 and 0.7). From Fig. 6, it can be observed:

- For a damping rate equals to 0.6, the measurement error value is less than or equal to 3.7%.
- For a damping rate equals to 0.63, the measurement error value is less than or equal to 2.2%.
- For a damping rate equals to 0.65, the measurement error value is less than or equal to 1.2%.

Table 2 Simulation parameters

Parameters	Value
Natural frequency of the accelerometer (Hz)	10,000
Damping rate	0.6, 0.63, 0.65, 0.68, 0.7
Relative frequency of vibratory motion (Hz)	0–4200
Movement amplitude (mm)	0.5

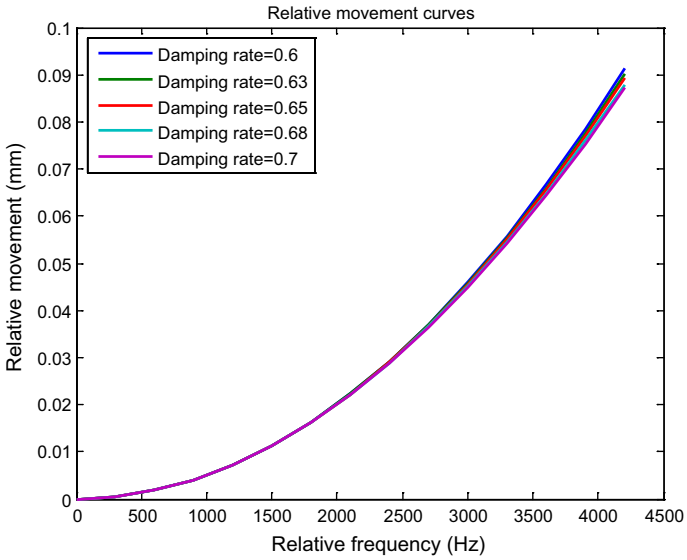

Fig. 7 Relative movement as a function of the relative frequency for various values of the damping rate

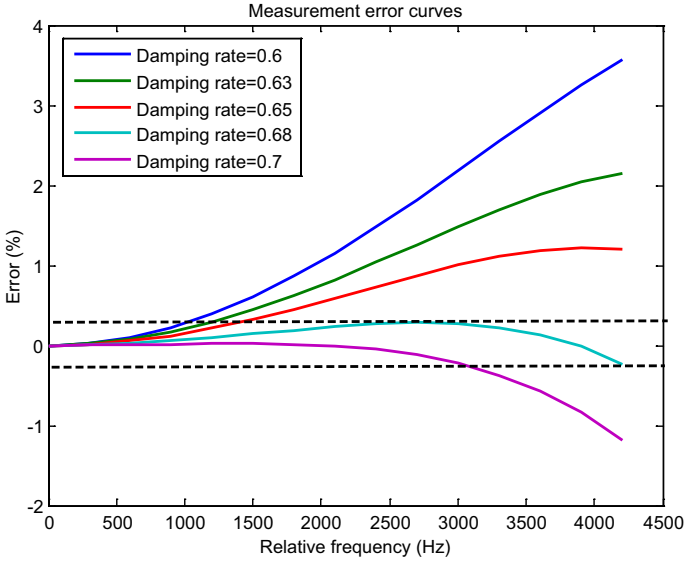

Fig. 8 Measurement error as a function of relative frequency for various values of damping rate

- For a damping rate equals to 0.68, the measurement error value is less than or equal to 0.3%.

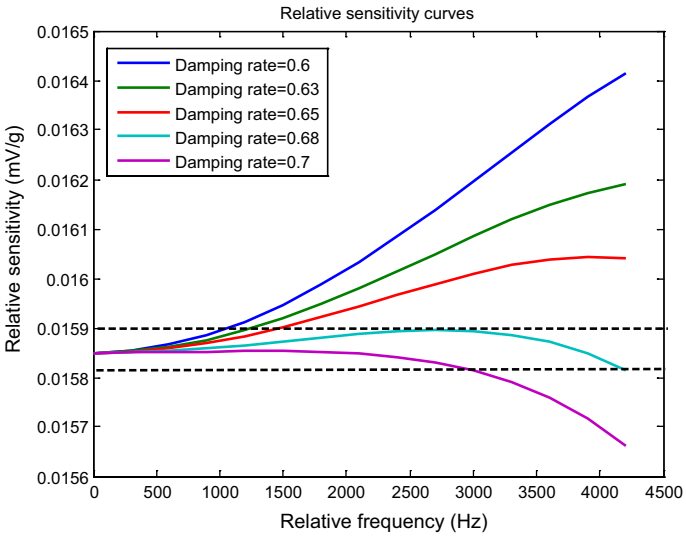

Fig. 9 Accelerometer relative sensitivity as a function of relative frequency for various values of the damping rate

- For a damping rate equals to 0.7, the measurement error value is less than or equal to 1.2%.

It can be also noted that the damping rate equal to 0.68 is the appropriate value to reduce the measurement error to a value not exceeding 0.3% and increasing the accelerometer precision to the maximum.

The simulation results of the new expression of relative sensitivity are presented in Fig. 9:

Figure 9 illustrates the piezoelectric accelerometer relative sensitivity as a function of relative frequency for five damping rate values. From this figure it can be noted that:

- For a damping rate equals to 0.6, the uncertainty of relative sensitivity is to $\pm 0.0005 \rightarrow (3.5\%)$.
- For a damping rate equals to 0.63, the uncertainty of relative sensitivity is to $\pm 0.00035 \rightarrow (2.2\%)$.
- For a damping rate equals to 0.65, the uncertainty of relative sensitivity is to $\pm 0.0002 \rightarrow (1.26\%)$.
- For a damping rate equals to 0.68, the uncertainty of relative sensitivity is to $\pm 0.00005 \rightarrow (0.35\%)$.
- For a damping rate equals to 0.7, the uncertainty of relative sensitivity is to $\pm 0.0002 \rightarrow (1.26\%)$.

With a damping rate equal to 0.68, it is possible to obtain a relative sensitivity slightly constant compared to others (a change in relative sensitivity does not exceed a value equal to 0.62%); this implies that the accelerometer is more sensitive. The selected value of damping rate (0.68) has improved the piezoelectric accelerometer parameters such as precision and relative sensitivity (measurement error minimization implies that the precision is optimized, and the sensitivity is enhanced).

7 Conclusion

In this work, the piezoelectric accelerometer and the piezoelectric material effect are studied to understand the structure and the operating principle of this type of sensor. Then an appropriate mathematical model of the physical behavior of this accelerometer is extracted. The developed model of the mechanical part shows two important formulas. The first is the expression of the relative movement as a function of the damping rate, the accelerometer natural frequency and the movement relative frequency. The second formula expresses the measurement error according to the parameters of the accelerometer, whereas, the new formula of the relative sensitivity relates the electrical and the mechanical parameters of the piezoelectric accelerometer. The developed model is validated by simulation tests and the obtained results have showed that a damping rate of 0.68 minimizes the measurement error to a value equal to 0.3%, increases the accuracy to a value equal to 99.7% and a change in relative sensitivity not exceeding a value of 0.62%. In future work, the fidelity and the availability of the piezoelectric accelerometer will be studied and a new will be proposed.

Acknowledgements The authors like to thank the Algerian general direction of research (DGRSDT) for their financial support.

References

1. Elfezazi, S. et al. (2003). Vers un outil, basé sur l'analyse fonctionnelle, pour la mise en œuvre des indicateurs de mesure de performance de la fonction maintenance. *Revue française de gestion industrielle, 22*(3), 1–15.
2. Gelders, L. et al. la gestion des pièces de rechange et la sous-traitance: quelques directives pratiques. *Revue Française de gestion industrielle, 22*(3), 1–10.
3. Molina, A. O. (2005). Méthodologie pour le placement des capteurs à base de méthodes de classification en vue du diagnostic, Doctorat de l'institut national des sciences appliquées de Toulouse.
4. Boulonger, A., & Pachaud, C. (1988). *Diagnostic vibratoire en maintenance préventive*. Paris: Dunod.
5. Des Forges, X. Méthodologie de surveillance en fabrication mécanique: Application de capteur intelligent à la surveillance d'une machine-outil. Thèse de Doctorat, Université Bordeaux I, Janvier 99.
6. Debray, K., Bogard, F., & Guo, Y.-Q. (2004). Numerical methodology to easily detect defects in revolving machines by vibration analysis. *Archive of Applied Mechanics, 74,* 45. https://doi.org/10.1007/bf02637208.

7. Dong S. –P., Yang, J., Fan, X. -W. (2017) Signal optimization of the AE piezoelectric sensor. In: *2017 Symposium on piezoelectricity, acoustic waves, and device applications (SPAWDA)*, Chengdu, China. https://doi.org/10.1109/spawda.2017.8340297. Accessed 27–30 Oct 2017
8. Hoshyarmanesh, H., & Maddahi, Y. (2017). Poling process of composite piezoelectric sensors for structural health monitoring: A pilot comparative study. *IEEE Sensors Letters, 2*(1), 1472–2475. https://doi.org/10.1109/lsens.2018.2806301.
9. Al Ahmad, M., & Ahmed, S. (2017). Heart-rate and pressure-rate determination using piezoelectric sensor from the neck. In *2017 4th IEEE international conference on engineering technologies and applied sciences (ICETAS)*, 29 Nov–1 Dec 2017. Salmabad, Bahrain, https://doi.org/10.1109/icetas.2017.8277911.
10. Booth, R., & Goldsmith, P. (2017). Detecting finger gestures with a wrist worn piezoelectric sensor array. In *2017 IEEE international conference on systems, man, and cybernetics (SMC)*, 5–8 Oct 2017, Banff, AB, Canada, https://doi.org/10.1109/smc.2017.8123202.
11. Kim, M.-K., & Yoon, S.-W. (2018). Miniature piezoelectric sensor for in-situ temperature monitoring of silicon and silicon carbide power modules operating at high temperature. *IEEE Transactions on Industry Applications, 54*(2), 1614–1621. https://doi.org/10.1109/tia.2017.2777923.
12. Mahbub, I., et al. (2015). A low-power wireless piezoelectric sensor-based respiration monitoring system realized in CMOS process. *IEEE Sensors Journal, 17*(6), 1858–1864. https://doi.org/10.1109/jsen.2017.2651073.
13. Ahmadi, S., & Azhari, S.-J. (2018). A novel fully differential second generation current conveyor and its application as a very high CMRR instrumentation amplifier. *Emerging Science Journal, 2*(2), 85–92. https://doi.org/10.28991/esj-2018-01131.
14. Omidi, A., Karami, R., Emadi, P.-S., & Moradi, H. (2017). Design of the low noise amplifier circuit in band L for improve the gain and circuit stability. *Emerging Science Journal, 1*(4), 192–200. https://doi.org/10.28991/ijse-01122.
15. Rezaee, M., Gisel, M.-N., & Saffari, S. (2017). Mathematical modeling and sensitivity analysis on cadmium transport in kaolinite under direct current electric field. *Civil Engineering Journal, 3*(11), 1097–1110. https://doi.org/10.28991/cej-030940.
16. Najafgholipour, M., & Soodbakhsh, N. (2016). Modified differential transform method for solving vibration equations of MDOF systems. *Civil Engineering Journal, 2*(4), 123–139.
17. Jahanirad, H., & Karam, H. (2017). BIST-based testing and diagnosis of LUTs in SRAM-based FPGAs. *Emerging Science Journal, 1*(4), 216–225.
18. Hu, J., Peng, H., Liu, T., Yao, X., Wu, H., & Lu, P. (2019). A flow sensing method of power spectrum based on piezoelectric effect and vortex-induced vibrations. *Measurement, 131,* 473–481. https://doi.org/10.1016/j.measurement.2018.08.020.
19. Danouj, B., Tahan, S. A., & David, E. (2013). Using a new generation of piezoelectric sensors for partial discharge detection. *Measurement, 46,* 660–666. https://doi.org/10.1016/j.measurement.2012.09.005.
20. Zhao, S., & Fu, H. (2018). A novel vibration sensor system for frequency measurement based on Bias Flip technique. *Measurement, 124,* 56–63. https://doi.org/10.1016/j.measurement.2018.03.070.
21. Noheda, B., Gonzalo, J. A., Cross, L. E., Guo, R., Park, S.-E., Cox, D. E., Shirane, G. (2000). Tetragonal-to-monoclinic phase transition in a ferroelectric perovskite: The structure of PbZr0.52Ti0.48O3. *Physical Review B, 61*(13), 1–18.